REPORT DOCUMENTATION PAGE

Form Approved
OMB No. 0704-0188

1. REPORT DATE *(DD-MM-YYYY)*	2. REPORT TYPE	3. DATES COVERED *(From - To)*
	Technical Papers	

4. TITLE AND SUBTITLE	5a. CONTRACT NUMBER
	5b. GRANT NUMBER
	5c. PROGRAM ELEMENT NUMBER
6. AUTHOR(S)	5d. PROJECT NUMBER
	5e. TASK NUMBER
	5f. WORK UNIT NUMBER

7. PERFORMING ORGANIZATION NAME(S) AND ADDRESS(ES)	8. PERFORMING ORGANIZATION REPORT
Air Force Research Laboratory (AFMC) AFRL/PRS 5 Pollux Drive Edwards AFB CA 93524-7048	
9. SPONSORING / MONITORING AGENCY NAME(S) AND ADDRESS(ES)	**10. SPONSOR/MONITOR'S ACRONYM(S)**
Air Force Research Laboratory (AFMC) AFRL/PRS 5 Pollux Drive Edwards AFB CA 93524-7048	**11. SPONSOR/MONITOR'S NUMBER(S)**

12. DISTRIBUTION / AVAILABILITY STATEMENT

Approved for public release; distribution unlimited.

13. SUPPLEMENTARY NOTES

14. ABSTRACT

15. SUBJECT TERMS

16. SECURITY CLASSIFICATION OF:			17. LIMITATION OF ABSTRACT	18. NUMBER OF PAGES	19a. NAME OF RESPONSIBLE PERSON
a. REPORT	b. ABSTRACT	c. THIS PAGE			Leilani Richardson
Unclassified	Unclassified	Unclassified	A		19b. TELEPHONE NUMBER *(include area code)* (661) 275-5015

41 items enclosed

3005[illegible]

TP-FY99-0150

✓ Spreadsheet
✓ DTJ

MEMORANDUM FOR PRS

FROM: PROI (TI) (STINFO) 11 June 1999

SUBJECT: Authorization for Release of Technical Information, Control Number: **AFRL-PR-ED-TP-FY99-0150**
D. Mueller et al. (ASI), "Recent ASI Progress in Pulse Detonation Rocket Engine (PDRE) Hardware Development"

AIAA JPC Paper **(Statement A)**

RECENT ASI PROGRESS IN PULSE DETONATION ROCKET ENGINE (PDRE) HARDWARE DEVELOPMENT

D. C. Mueller*, T. E, Bratkovich, K. Lupkes, S. Henderson, J. T. Williams, and T. R. A. Bussing

Abstract

This paper presents a brief overview of Adroit Systems, Inc., (ASI) experimental Pulse Detonation Rocket Engine (PDRE) development efforts and accompanying numerical modeling efforts. Test results for thirty-second firings of a H_2/O_2 fueled combustor at firing frequencies of up to 95 Hz are presented for a range of propellant mixture ratios. These experimental results were then used to validate a single-combustor computational model. The necessity of elevated operating pressure to engine performance is outlined. ASI efforts to obtain these elevated operating pressures are then briefly presented.

Introduction:

Potential performance improvements in conventional chemical propulsion systems are becoming increasingly difficult to obtain as propulsion technology is refined. Pulse Detonation Engines, both air-breathing and rocket-based, have received considerable attention over the past several decades due to possible performance improvements and/or reduced complexity when compared to these conventional chemical propulsion systems.[1, 2, 3, 4, 5, 6, 7, 8, 9, 10, 11, 12, 13, 14, 15, 16, 17, 18, 19]. Not until recently, however, has the pulse detonation propulsion concept been verifiably proven in a benchtop configuration.

In essence, the potential engine performance improvements associated with detonative operation can be traced to the lower entropy gain produced in a detonation when compared to a deflagration. As can be seen in Figure 1, given a specified initial condition, a detonation results in the lowest possible entropy state on the Hugoniot curve. This lower entropy gain may lead to improved performance if the entropy gain through the remainder of the engine is comparable to that in a conventional deflagrative system. ASI has been working to engineer a practical system that can generate these conditions within the constraints of mission level metrics such as cost, reliability, weight, and volume.

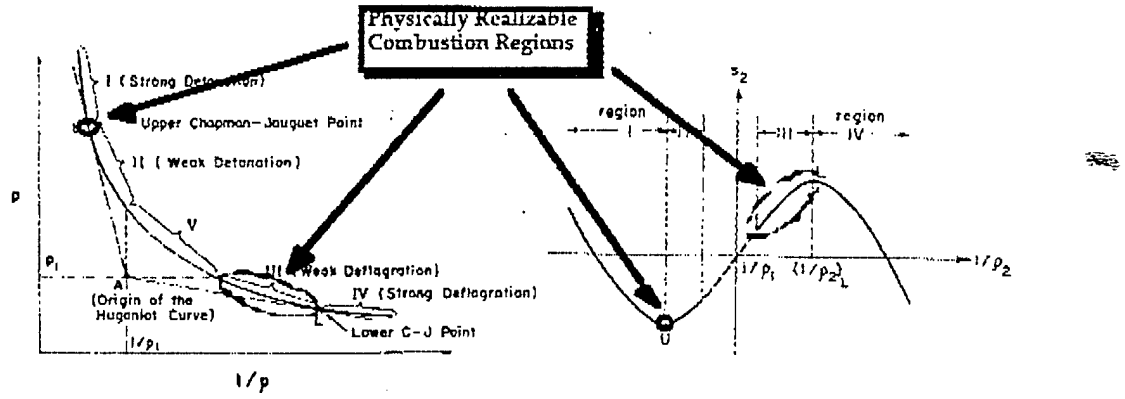

Figure 1: Hugoniot curve and resulting entropy for each point on the curve[20].

PDRE designs have been formulated around the core idea of cyclically initiating unsteady detonation waves in a series of combustion chambers[21]. The operation of a single combustor is depicted in Figure 2. Following the exhaust from the previous cycle, a gaseous purge buffer is injected into the combustor and the detonation chamber is charged with a fresh fuel/oxidizer mixture. The purge buffer is required to isolate the fresh charge from the hot combustion products of the previous cycle. A fast-acting valving system seals the chamber and detonation is initiated at the closed end by an initiation device. The detonation wave propagates through the combustor at supersonic velocities, and is followed by a series of rarefaction waves which ultimately propagate toward the combustor head as the burned gases exhaust from the combustor. During this time, the pressure at the upstream end

of the combustion chamber, known as P3, is several times that of the initial fill charge pressure. In a PDRE, P_3 can be ~6 - 12 times the initial fill pressure and can last for ~1-3 ms depending on the thermodynamic conditions of the fresh charge and combustor geometry. When the pressure within the combustor drops to an appropriate level, the purge and fresh fill processes are repeated.

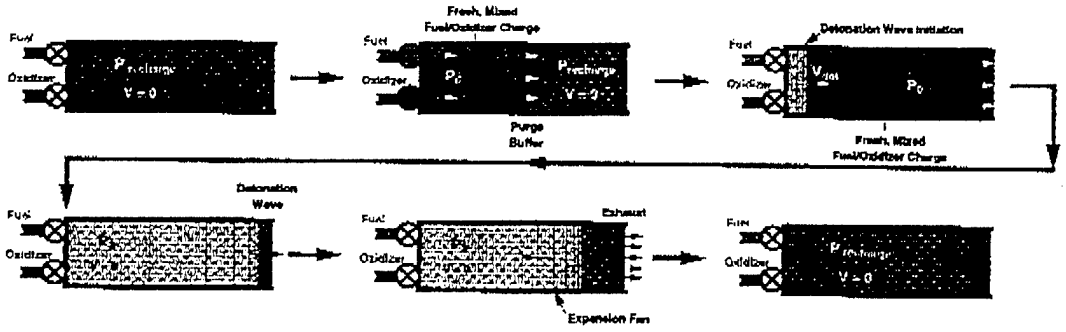

Figure 2: Schematic of basic combustor cycle operation.

Figure 3 presents a simplified conceptual drawing of the PDRE components. PDREs may be constructed in a variety of manners, however, the engine will typically consist of several separate detonation combustion chambers coupled to a propellant feed system, manifold, and nozzle. The combustors are cyclically fired in a phased manner, allowing the feed system and manifolds to operate in a steady state manner and the nozzle in a quasi-steady manner. PDREs may utilize a variety of conventional feed systems, including staged combustion, gas generator, expander, and pressure fed designs.

Important components include: feed system hardware (fuel and oxidizer pumps, gas generator(s)/preburners, cycle ducting and valves, etc.), fuel/oxidizer manifolds, flow metering valves that provide unsteady flow streams to the combustors via the steady flow manifolds, a detonation initiation system and controller, detonation combustors, a thermal protection system (TPS), a nozzle/combustor interface, and a well contoured nozzle. Although not shown in the figure, gimbal mounts, thrust vector control actuators, and power conditioning systems may also be present.

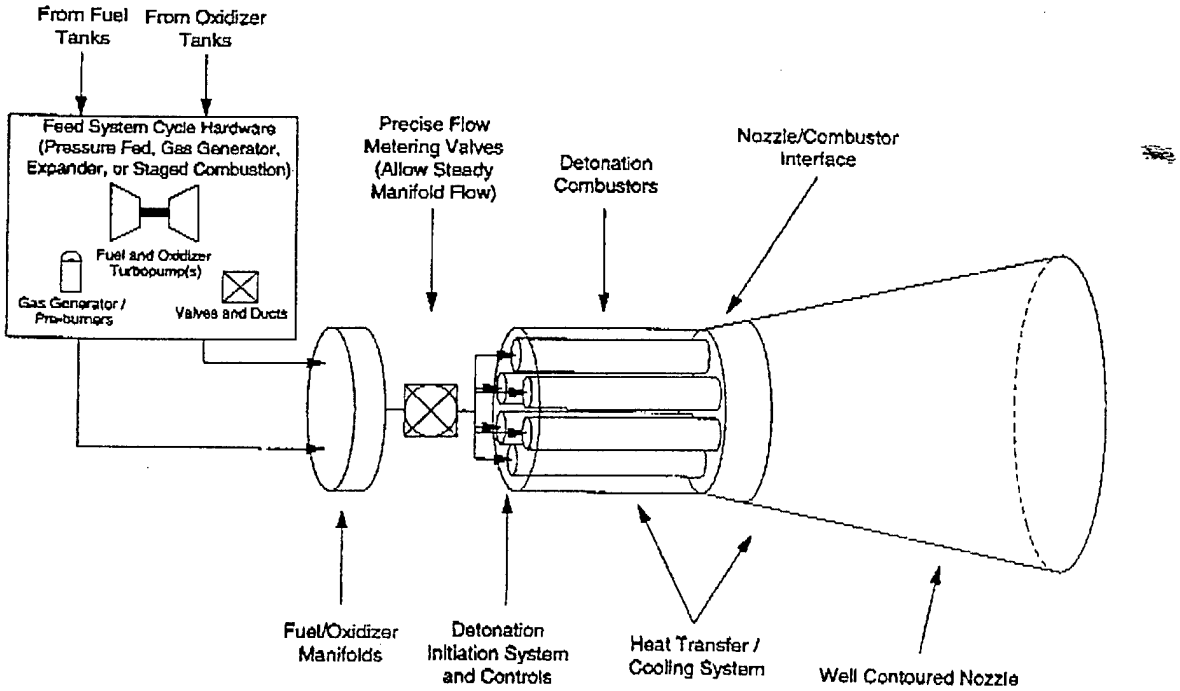

Figure 3. Pulse Detonation Rocket Engine component overview

PDRE Single-Combustor Experimental Testing

ASI constructed an uncooled single combustor test article that was operated successfully at frequencies up to 145 Hz and one second firing durations in the 1995 timeframe[21]. During the 1996-1997 period, ASI successfully tested a water-cooled, single-combustor test article that employed a gaseous hydrogen/oxygen propellant combination. This test article is shown in Figure 4. The test matrix covered propellant mixture ratios of 5.0 to 7.0 and thirty-second run durations were obtained at full-fill combustor firing frequencies of 95 Hz. Over 75 test firings were conducted and successful detonation percentages of 100% were obtained for all of the test cases presented in this paper. Detonative operation was verified through wavespeed and P_3 pressures measurements, obtained from fast-response piezoelectric pressure transducers and other instrumentation. A representative pressure trace from a thirty-second engine firing is presented in Figure 5 for one location in the chamber. Note that the variation in peak pressure from shot to shot is not the result of improper detonation, but rather, the low data sample rate (2 kHz) required to collect 30 seconds of data. This low sample rate effect was verified through comparison of high and low sample rate (1 MHz and 2 kHz) pressure traces taken during short duration testing. An expanded view of a representative pressure trace that was obtained using a 1 Mhz sample rate is shown in Figure 6. This trace displays the characteristics of a classical detonation pressure pulse; passage of the detonation wave, the expansion to the P_3 plateau pressure, and arrival of the upstream traveling rarefaction wave that signifies the exhaust of the chamber back to ambient conditions.

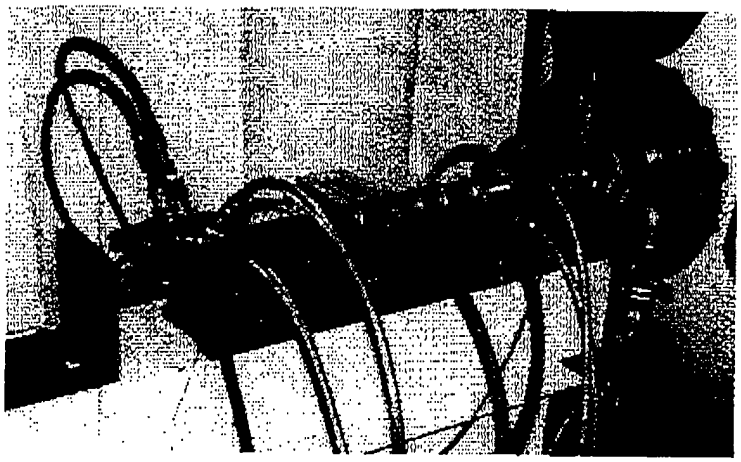

Figure 4: Water-cooled, gaseous H_2/O_2-fueled test article. Note that the combustor is approximately 36 inches long and has an internal diameter of approximately one inch.

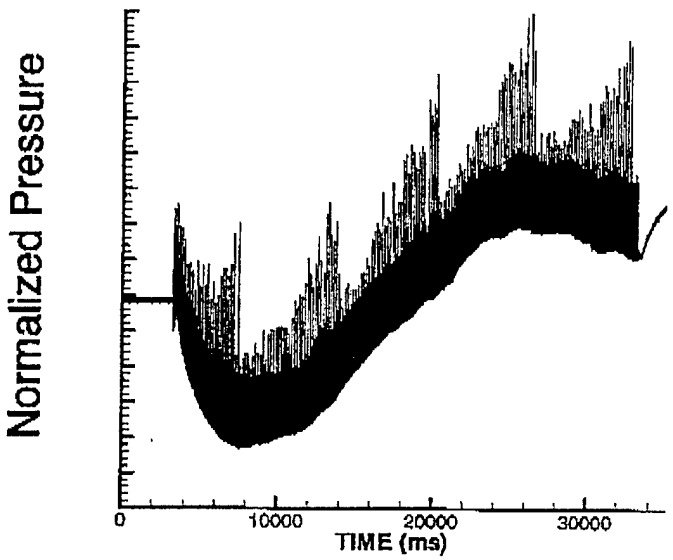

Figure 5: 30 second data trace##

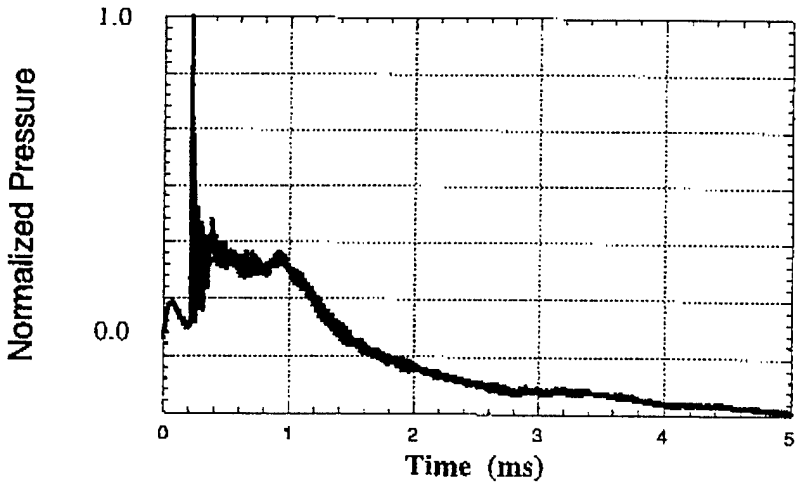

Figure 6: Blowup of one detonation pulse.

Combustor thrust, combustor wall temperatures, and water temperatures, and water flowrate were all measured as functions of propellant mixture ratio and firing frequency. In addition, propellant and purge mass flow rates were determined at each operating condition, permitting estimates of combustor I_{sp} to be obtained.

Combustor Wall Temperatures and Heat Transfer

The test article was primarily instrumented with thermocouples for health monitoring/safety reasons and to verify that thermal equilibrium operation was attained. However, the recorded temperature data also proved useful in estimating time-averaged combustor heat transfer characteristics.

The outer wall of the combustor was instrumented with intrinsic, fast-response, K-type thermocouples to permit time-dependent water-side wall temperatures to be recorded. As can be seen in Figure 7, these thermocouples were mounted in four pairs at different combustor axial locations. These thermocouples were connected to a health monitoring system that shutdown combustor operation if the temperatures exceeded nominal operating parameters. Thermocouples were also incorporated into the water cooling system, permitting time-accurate measurements of water temperature upstream and downstream of the test article.

The data from these wall and water thermocouples were used to verify that the combustor had attained operation at thermal equilibrium conditions and, given the water flowrate, to estimate the average heat transfer from the combustor to the cooling water. Representative, time-dependent combustor wall and exit water temperature traces are presented in Figure 8 for a thirty-second 95-Hz test firing at a mixture ratio of five. The wall temperature was measured 12 inches from the injector head. Note that these data clearly show that operation at combustor thermal equilibrium was obtained. Although not presented here, wall temperatures and overall combustor heat flux were evaluated over the mixture ratio and firing frequency range examined (MR = 5 to 7).

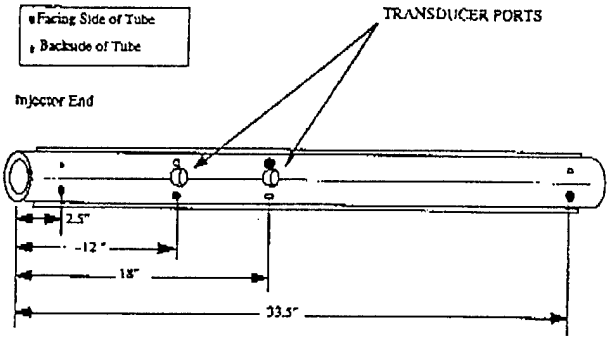

Figure 7: Location of K-type intrinsic thermocouples used to measure water-side combustor wall temperatures.

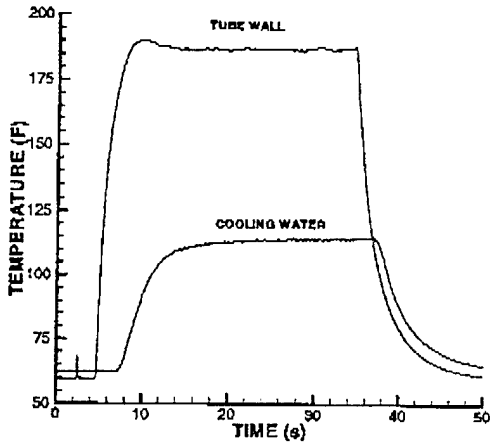

Figure 8: Water-side combustor wall and water exit temperatures as functions of time for an 80 Hz firing at a mixture ratio of five.

Combustor Thrust

Combustor thrust was measured as a function of combustor firing frequency and propellant mixture ratio using an ASI-proprietary thrust measurement system. Time-averaged thrust levels, depicted in Figure 9, were on the order of 10 lbf or less and thrust was found to increase in a near-linear fashion with combustor firing frequency, as would be expected. Thrust was also found to increase with decreasing propellant mixture ratio within the mixture ratio range examined.

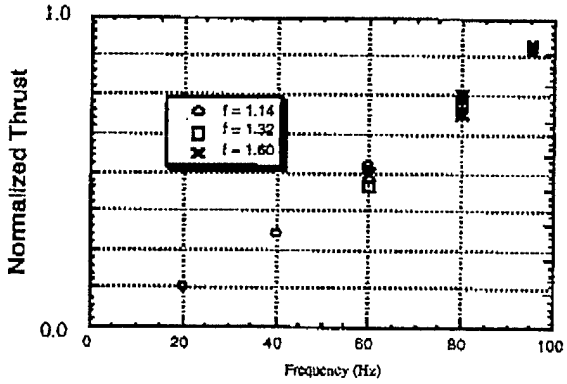

Figure 9: Time-average combustor thrust as a function of combustor firing frequency and propellant mixture ratio.

CFD Modeling of PDRE Wave Physics

MOZART2D Modifications

ASI acquired a version of the MOZART2D computational fluid dynamics (CFD) code[14] from an outside source. MOZART2D is designed to model full Navier-Stokes two-dimensional unsteady, reacting flows and has been used for pulse detonation work in the past[22, 23]. ASI had extensive experience with the operation and modification of a one-dimensional version of this code, which has been used extensively during past ASI PDE and PDRE development efforts to model both single and multiple cycle operation[24].

Several important modifications to the MOZART2D code were implemented, including event timing logic (to control simulation events), time-varying boundary conditions (to simulate valves opening and closing), fixed mass flow boundary conditions (to simulate choked gaseous propellant injection), time-varying flow property specification (to simulate spark ignition), time-varying multigrid capability (to reduce computational overhead), advanced moving subgrids (to reduce overhead associated with detonation resolution) and impulse and mass calculators (to facilitate

analysis). The new, modified code, known as ASIMOZ2D, has been utilized to model several ASI test articles and other envisioned future designs.

ASI constructed a representative two-dimensional Euler simulation (with finite rate chemistry) of the single chamber, water-cooled test article that was described above using ASIMOZ2D. The primary objectives of the modeling was to aid in the analysis of the data obtained during testing of the apparatus and to validate certain portions of the ASIMOZ2D code. The components of interest covered by the axisymmetric simulation are shown in Figure 10. Due to the cylindrical nature of each component, a rotational plane of symmetry exists along the center axis of the detonation chamber and dump tank.

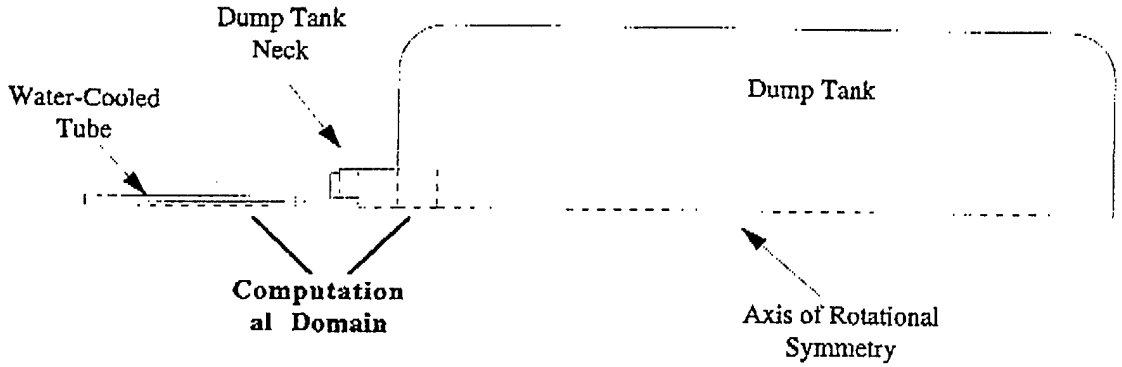

Figure 10: Apparatus Covered by the Single Tube CFD Simulation

The computational domain consisted of three fundamental components - the detonation tube, the neck of the dump tank, and the dump tank body, as shown in Figure 11 and Figure 12. Six different grids were used in the simulation to correctly capture the flowpath in the domain. The combustor internal flow path matched the actual geometry of the hardware, with the exception of the injector head. The injector head's complex geometry was modeled as a simple cylindrical section of equivalent volume. Thus, the localized mixing phenomena was neglected in the first inch or so of the chamber, which was determined to have little detrimental impact on the bulk accuracy of the model. Note also that only a small cylindrical region of the dump tank body was modeled (grid 5) in order to cut down on the computational overhead associated with the model. However, the dump tank neck and aft end of the tube were modeled in detail in an effort to capture the relevant flow characteristics in the vicinity of the tube exit.

Setup and Initial Conditions

An initial set of test cases were run to work out correct control timing and to identify regions of numerical instability. The upstream boundary condition was a solid free-slip wall to mimic the time when the valves were closed and the tube was detonating, while a fixed-mass-inflow boundary was utilized to simulate the injection of the gaseous propellants during the filling time. Note that this inflow BC was alterable to allow injection of pure hydrogen (the purge) or a pre-mixed charge of H_2/O_2. The aft boundary was modeled using a fixed pressure condition to simulate the large plenum volume of the dump tank. The initial conditions utilized for the simulation were chosen as representative of the final solution. Notice, however, that in all cases several full operational cycles were completed until a converged multi-cycle had been reached. The convergence criterion consisted of a sufficiently small deviation in the integrated impulse generated at the pressure surfaces from cycle to cycle.

The control algorithm for the model was as follows. At simulation start, the valve between the combustor and the upstream propellant manifold closed. The subgrid was initialized and activated at the entrance of the combustor. A numerical spark (region of high pressure and temperature) was generated in the first 5 cells of the subgrid. Detonation combustion ensued, and as the flame front continued down the chamber length, the subgrid moved so that the detonation was always captured. Note that the chemistry routines were activated *only* in the subgrid during the time when the detonation wave was traversing the chamber length to minimize computational overhead. This simplification was valid in that the detonation chemistry occurs over an exceedingly small time scale and distance. Thus, the flow after the passage of the detonation wave was essentially frozen. The code actively tracked the 2D location of the contact surface between the purge buffer and the fresh charge contact surface. When the detonation wave reached the aft-most location of the contact surface, the subgrid movement and flow calculations were turned

off. The simulation proceeded with the detonation blowdown until the valve open time was reached. At this time, the hydrogen purge inflow boundary condition was activated, and purge gas pushed out the remaining hot products. At the specified time, the hydrogen/oxygen fresh charge inflow condition was activated, and the tube filled at the desired mass flow rate. The cycle repeated when the valve closing time was reached. All of these events were controlled dynamically by the event timing algorithms. The timing for the events was chosen to mimic an existing set of experimental tests to aid in understanding important measured phenomena. A set of 80 Hz runs were chosen for this purpose.

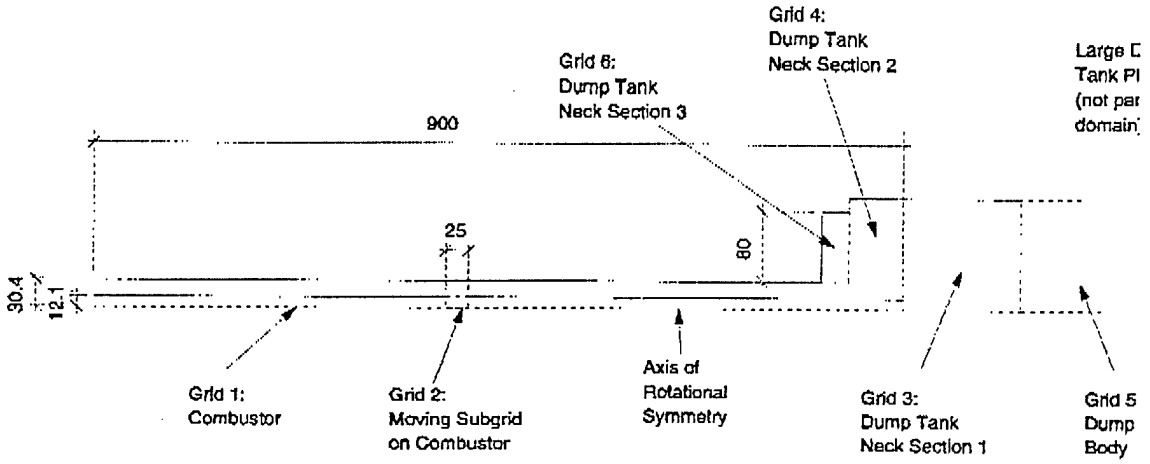

Figure 11: Computational Domain for the Water-Cooled Test Article Simulation. All Dimensions in mm

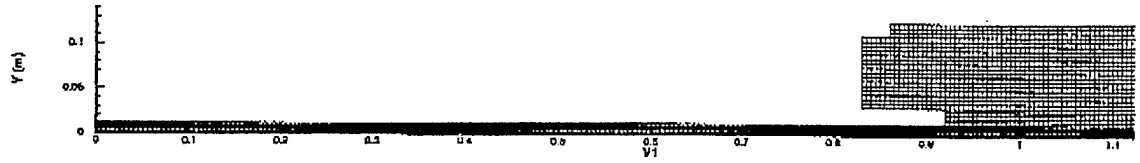

Figure 12: Computational Grid for Water-Cooled Test Article Simulation. Moving Subgrid Not Shown.

An initial trial was run from 0 - 62500 microseconds. At 80 Hz operation, the chamber experienced 5 complete detonation cycles during this time. Figure 13 shows the results plotted in the form of the pressure versus time at the valve center (i.e., along the center axis of the tube at the upstream end). The transient differences between each cycle are evident for the first three to four cycles, after which the simulation essentially reached a steady state of operation. The very narrow sharp peaks are associated with the numerical spark, and the large flat pressure profiles are characteristic of detonation combustion. Note that the standard, flat P_3 wall pressure that is evident for the first cycle of Figure 13 has some variation for later cycles, ending up with a value of ~6 atm. This variation was due to the detonation traveling through a uniform fuel/oxidizer slug specified by the initial conditions for the first shot, and to the variation of the fresh slug properties in two dimensions along the length of the chamber for succeeding shots. Note also that during the filling time, the pressure at the upstream end of the chamber oscillated as a series of expansion and re-compression waves traversed the chamber.

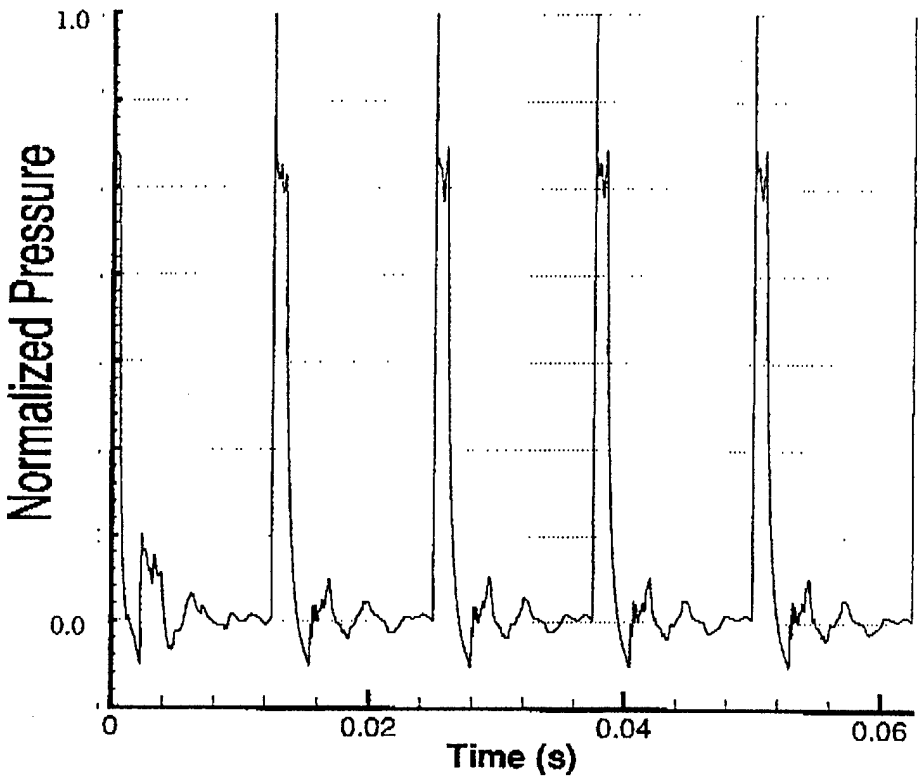

Figure 13: Pressure versus Time at the Valve Center (i.e., along the Center Axis of the Tube at the Upstream End) for 5 shots at 80 Hz

Analysis of Computed Time-Averaged Thrust and Isp

The performance characteristics of the detonation combustor for any given simulation were calculated by using the following equations:

$$F_{avr} = \frac{\text{Impulse}}{T_{cycle}} \qquad (1)$$

where F_{avr} is the time-averaged thrust, and T_{cycle} is the cycle time. Additionally,

$$Isp = \frac{F_{avr}}{\dot{m}_{avr} g} \qquad (2)$$

$$\dot{m}_{avr} = \dot{m}_{H_2\_avr} + \dot{m}_{O_2\_avr} \qquad (3)$$

where Isp is the specific impulse in seconds, $\dot{m}_{avr}$ is the time averaged mass flow processed during the cycle, $\dot{m}_{H_2\_avr}$ is the time averaged mass flow rate of hydrogen admitted to the chamber during each cycle (includes purge), $\dot{m}_{O_2\_avr}$ is the time averaged mass flow rate of oxygen admitted to the chamber during each cycle, and g is the gravitational constant. The impulse delivered to the tube is the sum of the pressure force at the thrust wall and that at the back edge of the tube exit in the dump tank:

$$\text{Impulse} = \text{Impulse}_{\text{thrust wall}} + \text{Impulse}_{\text{back edge}} \qquad (4)$$

Each of these impulses was calculated dynamically by the code during the simulation using the equations

$$\text{Impulse}_{\text{backedge}} = \sum_{i=i_{start}}^{i_{stop}} \sum_{j=\text{cell}_{\text{backedge}}} \left(P_j - P_{amb}\right)\left(\vec{n}_x \cdot \vec{A}_j\right) \cdot \Delta t_i \qquad (5)$$

$$\text{Impulse}_{\text{thrustwall}} = \sum_{i=i_{start}}^{i_{stop}} \sum_{j=\text{cell}_{\text{thrustwall}}} \left(P_j - P_{amb}\right)\left(\vec{n}_x \cdot \vec{A}_j\right) \cdot \Delta t_i \qquad (6)$$

where P_j absolute pressure in the computational cell, P_{amb} is the far field atmospheric pressure, $\vec{n}_x$ is the unit normal vector in the x-direction, $\vec{A}_j$ is the differential area of the cell face, and Δt_i is the discretized time step. The variables i_{start} and i_{stop} represent the iteration number between the beginning and end of a given cycle. Additionally, the variable "cell" represents the computational cells of the appropriate wall of interest. Note that the thrust wall force computed dynamically by the simulation included a small error (less than 1%) due to the presence of the numerical high pressure spark used to initiate the detonation. This value may be accounted for in the thrust calculations by subtracting the impulse generated from the spark from the computed value.

The time averaged mass flow rate of hydrogen and oxygen processed during one simulation cycle is,

$$\dot{m}_{H_2\_avr} = \frac{\int_{t=t_{start}}^{t_{stop}} \dot{m}_{H_2} \cdot dt}{T_{cycle}} \qquad (7)$$

$$\dot{m}_{O_2\_avr} = \frac{\int_{t=t_{start}}^{t_{stop}} \dot{m}_{O_2} \cdot dt}{T_{cycle}} \qquad (8)$$

and the cycle time is simply,

$$T_{cycle} = t_{start} - t_{stop} \qquad (9)$$

Several cases were run to explore the impact of the experimental variables. The first simulation used a 14.7 psia back pressure in the dump tank, which was typical of the initial shots of a multi-cycle test. However, ASI test engineers documented that the dump tank underwent a slight pressure rise of 0.2 psia during long duration runs, with a nearly steady value of 14.9 psia seen after approximately 3-5 seconds of operation. Therefore, other simulations were run using a dump tank back pressure of 14.9 psia to assess the trends in thrust production. It is notable that the CFD predicted a small negative thrust contribution from the back edge of the tube with a 14.7 psia tank pressure of approximately -8% of the total thrust generated. However, with a 14.9 psia tank pressure, the back edge of the tube provided a positive thrust contribution of approximate +5% of the total.

CFD Results Comparison to Analytic Model

A comparison of analytic model predicted results to the current CFD simulation of the test article was made. The simplified analytic model equations that were defined in previous ASI work[25] require that the chamber fresh charge filling Mach number be specified just before the detonation is initiated. However, the CFD simulations showed that this parameter varied down the axial length of the tube due to the presence of unsteady waves. Therefore, it was appropriate to bracket the fresh charge Mach number by running the analytic model with both the upper and lower pre-detonation chamber fill Mach number seen in the chamber CFD simulation.

Figure 14 and Figure 15 show the qualitative results of the comparison, where the second plot is an expanded view of the detonation over-pressure and exhaust rarefaction at the thrust wall. The analytic model bracketed the thrust wall overpressure well, and due to the model simplicity, essentially atmospheric pressure is predicted in the chamber after ~0.0015 seconds (for this single combustor, no nozzle geometry).

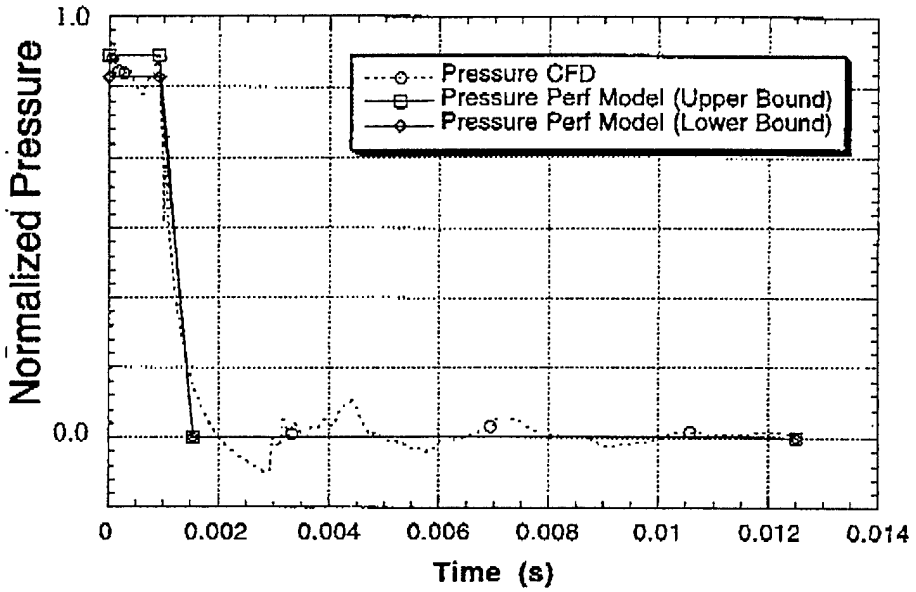

Figure 14: Comparison of the CFD and Analytic Model Predictions of Pressure at the Thrust Wall

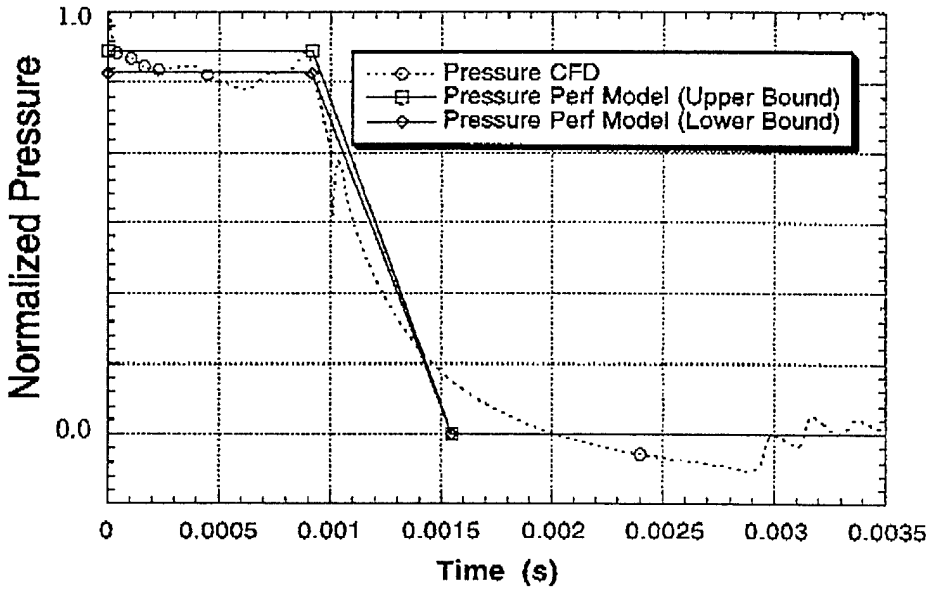

Figure 15: Expanded View of the Detonation Overpressure and the Exhaust Rarefaction (CFD Simulation and Analytic Model Prediction) at the Thrust Wall

Quantitative results of the comparison are shown in Table 1. The portion of the analytic model of interest here predicts only the chamber thrust wall pressure forces, therefore, the comparable thrust and Isp values for the CFD simulation do not include the back edge force contribution, nor do they include the purge mass decrement. The table shows that the analytic model predictions provide good agreement with the CFD calculated values. This comparison provides some measure of confidence that the analytic model, when extrapolated into more realistic flight conditions and engine configurations, provides a reasonable prediction of PDRE combustor performance. Note however, that flight configuration PDRE performance cannot be calculated by assessing the thrust produced in the combustor only, but must take into account all engine components as per CPIA 246 [26].

Table 1. Comparison of CFD Simulation and ASI Analytic Model Predictions, Single Combustor Operating at 80 Hz with No Nozzle Geometry

Case	Fresh Charge Fill Mach Number	Dump Tank Back Pressure (psia)	$F_{avr\ thrust\ wall}$ (Δ%)	Isp (Δ%)
CFD	0.28 < M(x) < 0.40	14.7	–	–
Performance Model: Upper Bound	0.28	14.7	-5.1%	+0.5%
Performance Model: Lower Bound	0.40	14.7	+0.9%	+7.0%
CFD	0.28 < M(x) < 0.32	14.9	–	–
Performance Model: Upper Bound	0.28	14.9	-7.8%	-7.1%
Performance Model: Lower Bound	0.32	14.9	-6.8%	-2.0%

Comparison of CFD to Experimental Results

A similar comparison was conducted between the CFD model results and the experimental data. Quantitative results of the comparison are shown in Table 2. The simulation results of interest here are those that reflect test conditions, such as the 14.9 psia dump tank pressure and inclusion of the force on the back edge of the tube. The table shows that the CFD simulation provides good agreement with the collected test data, and is within the bounds of the error inherent to both methodologies.

Table 2. Comparison of CFD Simulation and Single Chamber Test Data: 80 Hz, MR = 6.0, No Nozzle Geometry, 14.9 psi Dump Tank Pressure, Tube Back Edge Force Included.

Case	$F_{avr\ thrust\ wall}$ (Δ%)	Isp (Δ%)
Test	–	–
CFD	-3.8%	+2.0%

ASI has substantially improved the state-of-the-art in CFD modeling of pulse detonation propulsion systems in early 1997 by conducting the first known converged multi-cycle, two-dimensional simulations of pulse detonation combustors. The single chamber simulations showed good agreement with measured time-averaged thrust and dynamic pressure loading. Continued CFD modeling activities have allowed ASI to understand and visualize the flowfields of several test articles and integrated configurations before they were actually constructed and built, thus vastly reducing the design time and costs.

Multi-Combustor Experimental Testing

Conventional rocket engines require pressurization of the combustion chamber to obtain high performance. This may be simply seen by exercising ODE, CEA, or one of a host of other simplified first-law analysis codes that compute conventional rocket engine performance. Figure 16 shows the results of one such calculation for an ideal conventional rocket engine utilizing constant pressure combustion of hydrogen/oxygen propellants at a mixture ratio of 6.0 and expansion of the products to sea level pressure. The thermodynamics of the cycle analysis dictate that higher performance is obtained as the chamber pressure is increased. This fundamental trend in rocket propulsion performance is reflected in the trend seen in today's flight capable systems and the utilization of increasingly powerful turbopumps and feed systems to achieve higher performance.

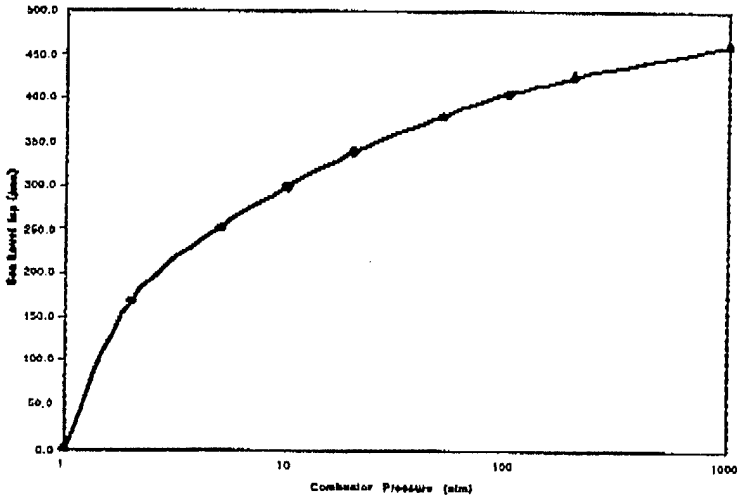

Figure 16: Conventional Rocket Engine Performance Calculations for H_2/O_2 Propellants at MR = 6.0 and Optimal Expansion to Sea Level Pressure.

A similar situation exists for pulse detonation rocket engines. Regardless of the combustion process and whether the flow is steady or unsteady, fundamental thermodynamics dictates that elevated combustor fill pressures must be achieved to obtain realistic performance levels in a flight capable rocket application. This holds true for detonation combustion rocket engines, although the detailed thermodynamic analysis is beyond the scope of this paper. Given this requirement, ASI has been investigating various combustor pressurization mechanisms and has developed a nozzle concept in which multiple combustors exhaust through a common nozzle flowpath.

A numerical and experimental investigation of this flowpath concept was initiated in the Fall of 1997. As part of this investigation, a water-cooled, six-combustor test article was constructed and tested at ambient and elevated fill pressures with hydrogen/oxygen propellants. A photograph of this test article in operation at a USAF AFRL test facility can be found in Figure 17. During the summer of 1998 under joint funding from ASI, NASA MSFC, and the USAF AFRL, over 250 test firings were conducted at a variety of propellant mixture ratios (5.1-7.4) and combustor fill pressures. Combustor firing frequencies of 80 Hz, corresponding to an engine frequency of 480 Hz, were obtained for firing durations of up to 10 seconds. As part of this effort, detonation pressures, combustor fill pressures, thrust, and test article wall temperatures were all recorded as functions of time. Combustor fill pressure is presented as a function of combustor firing frequency for mixture ratios of 5.1 and 7.4 in Figure 18. Work continues with this and other test articles to validate key operational and performance issues for PDREs.

Figure 17: Water-cooled, six-combustor test article shown in an ambient-pressure test firing.

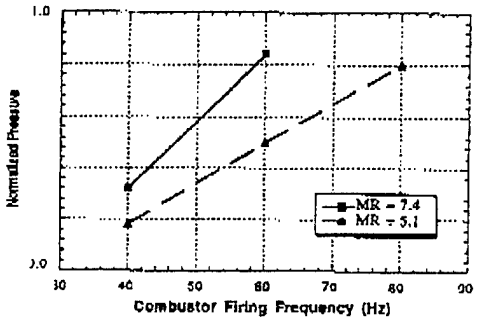

Figure 18: Combustor fill pressure as a function of engine firing frequency for mixture ratios of 5.1, and 7.4.

Conclusions

ASI has demonstrated high-frequency, long duration operation of a H_2/O_2 fueled PDRE combustor test article for a range of propellant mixture ratios. The results were used to benchmark a CFD numerical tool, and demonstrated fundamental proof-of-concept for PDRE combustors at an early technology readiness level. The necessity of elevated operating pressure to engine performance was outlined, and ASI efforts to obtain these elevated operating pressures with a multiple chamber design utilizing a common nozzle were briefly presented. ASI continues to retire risks associated with critical PDRE components through on-going research and development programs.

Acknowledgements

Portions of this work were funded by the U.S. Air Force and NASA. The authors would like to thank Dr. Bill Larson, Dr. Phil Kessel, Dr. Doug Talley, Dr. Ed Coy, and Dr. Steve Rodgers of the USAF AFRL and Mr. John Cole, Mr. Shayne Swint, Mr. John Price, and Mr. Garry Lyles of NASA-MSFC for their support. Additionally, the authors would like express their gratitude to members of ASI-AASD for their contributions to the efforts described herein.

References

1 Bussing, T.R.A. and Pappas, G., "An Introduction to Pulse Detonation Engines," AIAA 94-0263, 32nd AIAA Aerospace Sciences Meeting & Exhibit, Reno, NV, January 10-13, 1994.

2 Bussing, T. R. A., "A Rotary Valve Multiple Combustor Pulse Detonation Engine (RVMPDE)", AIAA 95-2577, 31st AIAA/ASME/SAE/ASEE Joint Propulsion Conference, San Diego, CA, July 10-12, 1995.

3 Hinkey, J.B., Bussing, T.R.A., and Kaye, L., "Shock Tube Experiments for the Development of a Hydrogen-Fueled Pulse Detonation Engine," AIAA 95-2578, 31st AIAA/ASME/SAE/ASEE Joint Propulsion Conference, San Diego, CA, July 10-12, 1995.

4 Ting, J.M., Bussing, T.R.A., and Hinkey, J.B., "Experimental Characterization of the Detonation Properties of Hydrocarbon Fuels for the Development of a Pulse Detonation Engine," AIAA 95-3154, 31st AIAA/ASME/SAE/ASEE Joint Propulsion Conference, San Diego, CA, July 10-12, 1995.

5 Bussing, T. R. A., Hinkey, J. B., and Kaye, L., "Pulse Detonation Engine Preliminary Design Considerations," AIAA 94-3220, 30th AIAA/ASME/SAE/ASEE Joint Propulsion Conference, Indianapolis, IN, June 27-29, 1994.

6 Bussing, T.R.A, Bratkovich, T.E., "Characteristics of Pulse Detonation Engines," 1995 JANNAF Propulsion and Joint Subcommittee Meetings, Tampa, FL, 4-8 December, 1995.

7 Bratkovich, T.E., and Bussing, T.R.A., "A Pulse Detonation Engine Performance Model," AIAA Paper 95-3220, 31st AIAA/ASME/SAE/ASEE Joint Propulsion Conference, San Diego, CA, July, 1995.

8 Aarnio, M.J., Hinkey, J.B., and Bussing, T.R.A., "Multiple Cycle Detonation Experiments During the Development of a Pulse Detonation Engine," AIAA Paper 96-3263, 31st AIAA/ASME/SAE/ASEE Joint Propulsion Conference, Lake Buena Vista, FL, July, 1996.

9 Eidelman, S., Grossmann, W., Lottati, I., "A Review of Propulsion Applications of the Pulsed Detonation Engine Concept", AIAA Paper 89-2446, July 10-12, 1989.

10 Eidelman, S., Grossman, W., Gunners, N.-E., and Lottati, I., "Progress in Pulsed Detonation Engine Development," AIAA Paper 94-2721, 1994.

11 Helman, D., Shreeve, R.P., Eidelman, S., "Detonation Pulse Engine", AIAA Paper 86-1683, 1986.

12 Krzycki, L.J., "Performance Characteristics on an Intermittent-Detonation Device," NAVWEPS Report 7655, AD-284312, U.S. Naval Ordnance Test Station, China Lake, California, June 1962.

13 Nicholls, J.A., Wilkinson, H.R., and Morrison, R.B., "Intermittent Detonation as a Thrust-Producing Mechanism," Jet Propulsion, Vol. 27, May, 1957.

14 Cambier, J. L., Adelman, H.G., "Preliminary Numerical Simulations of a Pulsed Detonation Wave Engine", AIAA Paper 88-2960, July 11-13, 1988.

15 Sterling, J., Ghorbanian, K., and Sobota, T., "Enhanced Combustion Pulsejet Engines for Mach 0 to 3 Applications," AIAA 96-2687, 32st AIAA/ASME/SAE/ASEE Joint Propulsion Conference, Lake Buena Vista, FL, July 1 - 3, 1996.

16 Lynch, E.D., Edelman, R., and Palaniswamy, S., "Computational Fluid Dynamic Analysis of the Pulse Detonation Engine Concept," AIAA 94-0264, 32nd AIAA Aerospace Sciences Meeting & Exhibit, Reno NV, January 10-13, 1994.

17 Hoffman, H., Reaction Propulsion by intermittent Detonative Combustion," Ministry of Supply, 1941.

18 Nicholls, J. A., Wilkinson, H. R., and Morrison, R. B., "Intermittent Detonation as a Thrust-Producing Mechanism," *Jet Propulsion*, Vol. 27, 1957, pp 534-541.

19 Nicholls, J.A., Cullen, R.E., and Ragland, K.W., "Feasibility Studies of a Rotating Detonation Wave Rocket Motor," Journal of Spacecraft, Vol. 3, No. 6, June, 1966.

20 Kuo, K.K., Principles of Combustion, John Wiley & Sons, 1986.

21 Bratkovich, T.E., Aarnio, M.J., Williams, J., and Bussing, T. R. A., "An Introduction to Pulse Detonation Rocket Engines," AIAA Paper 97-2742, 33rdAIAA/ASME/SAE/ASEE Joint Propulsion Conference & Exhibit, *1997.*

22 Cambier, J.-L., Adelman, H.G., and Menees, G.P., "Numerical Simulations of a Pulsed Detonation Wave Augmentation Device," *AIAA 93-1985, 29th AIAA/ASME/SAE/ASEE Joint Propulsion Conference & Exhibit*, June 28-30, 1993, Monterey, CA.

23 Cambier, J.-L., and Tegner, J.K., "Strategies for PDE Performance Optimization," *AIAA 97-2743, 33rd AIAA/ASME/SAE/ASEE Joint Propulsion Conference & Exhibit*, July 6-9, 1997, Seattle, WA.

24 Bratkovich, T., and Aarnio, M., *A Novel Hydrogen Fueled Propulsion System*, SBIR Phase II Final Report Add-on, Contract NAS1-20191 Performed for NASA LaRC, Adroit Systems, Inc., October 4, 1996.

25 Bratkovich, T., and Bussing, T.R.A., "A Pulse Detonation Engine Performance Model," *AIAA 95-3155, 31st AIAA/ASME/SAE/ASEE Joint Propulsion Conference & Exhibit*, July 10-12, 1995, San Diego, CA.

26 Chemical Propulsion Information Agency (CPIA), *JANNAF Rocket Engine Performance Predictions and Evaluation Manual*, CPIA Publication 246, 1975.